Clinical Case Reports Open Access WILEY

Family with congenital contractural arachnodactyly due to a novel multiexon deletion of the *FBN2* gene

Hiroki Yagi[1,2] | Hiroshi Takiguchi[1] | Norifumi Takeda[1,2] (ORCID) | Ryo Inuzuka[2,3] |
Yuki Taniguchi[2,4] | Kristine Joyce Porto[5] | Hiroyuki Ishiura[5] | Jun Mitsui[5] |
Hiroyuki Morita[1] | Issei Komuro[1]

[1]Department of Cardiovascular Medicine, The University of Tokyo Hospital, Tokyo, Japan

[2]Marfan Syndrome Center, The University of Tokyo Hospital, Tokyo, Japan

[3]Department of Pediatrics, The University of Tokyo Hospital, Tokyo, Japan

[4]Department of Orthopedic Surgery, The University of Tokyo Hospital, Tokyo, Japan

[5]Department of Neurology, The University of Tokyo Hospital, Tokyo, Japan

Correspondence
Norifumi Takeda, Department of Cardiovascular Medicine, The University of Tokyo Hospital, 7-3-1 Hongo, Bunkyo-ku, Tokyo 113-8655, Japan.
Email: norifutakeda@gmail.com

Abstract

Congenital contractural arachnodactyly (CCA) is caused by pathogenic *FBN2* variants; however, the contributions of copy number variations (CNVs) to CCA are still unknown. Here, we report on a familial case of CCA, in which a novel multiexon deletion of exons 35–39 in *FBN2* was identified after simple CNV prediction.

KEYWORDS

array-CGH, Beals syndrome, camptodactyly, copy number variation, integrative genomics viewer

1 | INTRODUCTION

Congenital contractural arachnodactyly (CCA), also known as Beals syndrome, is an autosomal-dominant heritable disorder of the connective tissue caused by pathogenic variants of the *FBN2* encoding fibrillin-2, a component of extracellular matrix microfibrils,[1,2] located at chromosome 5q23.3. CCA patients have a marfanoid habitus characterized by long slim limbs (dolichostenomelia) and long spider-like fingers (arachnodactyly) and thus, CCA must be differentiated from Marfan syndrome (MFS), which is caused by pathogenic variants in *FBN1*

encoding fibrillin-1. *FBN1* and *FBN2* are highly homologous genes with 65 coding exons, and both fibrillins are similarly expressed in most adult tissues but seem to differently contribute to extracellular matrix (ECM) functions.[3] Of the two cardinal features of MFS, aortic dilatation and/or dissection has rarely been observed, and ectopia lentis has never been documented in CCA, and CCA patients are more likely to exhibit flexion contracture of their fingers (camptodactyly) and external ear abnormalities such as a crumpled appearance of the ear helix. However, it is often difficult to diagnose differentially these hereditary disorders of connective tissue in clinical settings, and therefore,

---

Hiroki Yagi and Hiroshi Takiguchi contributed equally to this work.

the genetic testing can provide useful information when deciding a follow-up care plan.

Most *FBN2* pathogenic variants cluster within a limited region (exons 22–36), known as a hot spot, and pathogenic variants are evenly distributed as missense (50%) and splice-site variants (46.9%).[2] Recently, Meerschaut et al.[4] reported three CCA patients (6.8%) with multiexonic deletions among 44 *FBN2*-positive CCA patients; however, the significance of additional copy number analysis in CCA has not yet been established. Here, we present a Japanese familial case of CCA in which a novel heterozygous deletion affecting exons 35–39 in *FBN2* gene was identified by the copy number analysis, using a visual review of patterns of sequencing coverage in the Integrative Genomics Viewer (IGV) browser[5] and subsequent array comparative genomic hybridization (array-CGH) analysis.

2 | MATERIALS AND METHODS

2.1 | Genetic analysis

The genetic analysis of MFS-related disorders was approved by the University of Tokyo Hospital ethics committee (G-1538). Hybridization capture-based gene-panel testing for hereditary thoracic aortic aneurysm and dissection (HTAAD) was conducted at the Kazusa DNA Research Institute (Chiba, Japan).[5] The next-generation sequencing (NGS) panel included the genes *FBN1*, *FBN2*, *TGFBR1*, *TGFBR2*, *SMAD3*, *TGFB2*, *TGFB3*, *ACTA2*, *MYH11*, *MYLK*, *COL3A1*, *EFEMP2*, *FLNA*, and *SLC2A10*. The positions of the nucleotide sequences described in this report were based on the Genome Reference Consortium Human Build 38 Organism (GRCh38). Protein Variation Effect Analyzer (PROVEAN), a software tool that predicts to what extent an amino acid substitution or indel has an impact on the biological function of a protein (provean.jcvi.org/index/php), was selected for pathogenicity prediction. Data on the clinical phenotypes were collected by the staff of the Marfan syndrome center at our institute. Written informed consent was obtained from the patient.

2.2 | Copy number variation screening

For exome/panel sequence-based copy number variation (CNV) evaluation, the depth of coverage (*doc*) patterns of the exon of interest and neighboring exons were compared *via* visual inspection of the coverage tracks from the IGV browser.[5,6] We compared the sample of proband (#606) with four samples with close collection dates. To understand the overall trend of *doc* patterns throughout a gene,

the read depth (RD) of each exon was extracted using the ExomeDepth software[7] and visualized using Excel 2D line charts. To correct for the substantial differences in RDs, the RD for each was normalized by dividing it by the average of all RDs of the gene.

2.3 | Array-CGH

An Agilent 60-mer oligonucleotide-based CGH microarray (Agilent Technologies) was custom designed according to a previously published algorithm.[8] The microarray had 44,305 probes covering 15 genes causative for HTAAD as follows: *FBN1*, *FBN2*, *TGFBR1*, *TGFBR2*, *SMAD2*, *SMAD3*, *TGFB2*, *TGFB3*, *ACTA2*, *MYH11*, *MYLK*, *PRKG1*, *LOX*, *COL3A1*, and *SKI*. The average space between probes was 185 bp. The array-CGH was conducted following the manufacturer's protocols and analyzed using the Agilent CytoGenomics software (v5.1.1) with the default calling algorithm, as previously described.[5] Breakpoint mapping by PCR was used to confirm and refine the array-determined CNV candidate within the *FBN2* gene. The primers for the PCR were designed using the Primer3 software[9] to amplify over the breakpoint regions as follows: FBN2-Fw, 5′-CCC CAA CAC AAT AAA AGA CAC CT-3′ (128,320,104–128,320,082) and FBN2-Rv, 5′-AGC TGC TGG TTG TTC TCC TC-3′ (128,310,589–128,310,608).

2.4 | Patients

The proband (II-3; #606) was a 35-year-old Japanese woman with no apparent relevant family history, with suspected MFS in childhood, because of the presence of her spider-like fingers, left inguinal hernia, scoliosis, and mitral valve prolapse (Figure 1A). She underwent posterior spinal fusion surgery for scoliosis at the age of 13 (Figure 1B), and had been instructed to limit her participation in athletic activities during school days. At the age of 29, she was referred to our Marfan syndrome center for follow-up care. Her height and weight were 167 cm and 50 kg, respectively, and her arm span was 173 cm (span/height = 1.04). She had arachnodactyly with mild camptodactyly (Figure 1C), and showed positive thumb sign, pectus excavatum, left hindfoot deformity, reduced elbow extension, dural ectasia, and mild mitral valve prolapse. Her ear appearance was normal. She had a systemic score ≥7 points on the systemic feature scoring table for MFS[10]; however, transthoracic echocardiography revealed no dilatation of the sinuses of Valsalva, measuring 30 mm (Z-score = 1.23)[11] and her intraocular lenses were not dislocated; she did not clinically fulfill the revised Ghent criteria for MFS.

3 | RESULTS

We performed genetic analysis of the proband at the age of 35, when the camptodactyly was passed on to her second daughter (III-2) (Figure 1A). NGS panel testing for HTAAD was conducted; however, no pathogenic or likely pathogenic variants and/or variants of uncertain significance were still identified. Recently, we have reported the significance of CNV in syndromic aortopathies[5]; therefore, we next simply predicted CNVs *via* visual review of the *doc* patterns of NGS panel testing data (Figure 2). Three independent inspectors finally called a suspected heterozygous deletion of exons 35–39 of the *FBN2* gene, in which she had a patient/control *doc* ratio of approximately 0.5. Array-CGH analysis revealed an 8.4-kb deletion within the *FBN2* gene, which was flanked by oligomer CG_j200786_0037632 (128,311,268–128,311,327) to oligomer CG_j200786_0037664 (128,319,585–128,319,644) and encompassed exons 35–39. Using primers flanking the breakpoint, the deleted allele was preferentially amplified over the larger normal allele (Figure 3A). Subsequent sequence analysis of the mutant allele identified an 8833 bp deletion with intronic breakpoints at chr5:128,310,832 in intron 39 and at chr5:128,319,664 in intron 34 within the *FBN2* gene (NC_000005.10:g.128310 832_128319664del) (Figure 3B). This deletion is predicted to result in an in-frame loss of exons 35–39 at transcription level (NM_001999.4:c.4472_5074del) and produce an internally truncated fibrillin-2 protein (NP_001990.2:p. Ser1496_Cys1696del). This deletion variant is absent
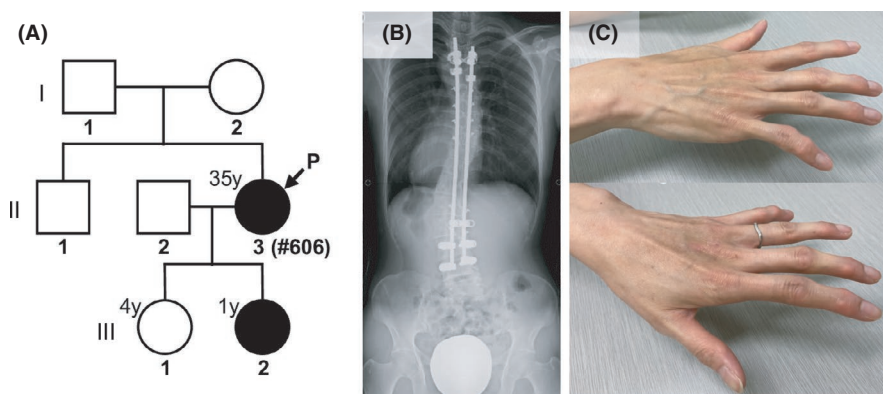

FIGURE 1 Japanese familial case of CCA. (A) One pedigree with finger contracture (camptodactyly) in this study. Age is shown in the upper left corner. Square, male; circle, female; arrow, proband; solid, affected by camptodactyly; open, unaffected by camptodactyly. (B) Postoperative posteroanterior radiograph of the spine showing severe scoliosis in the proband (II-3, #606). (C) Camptodactyly in the proband
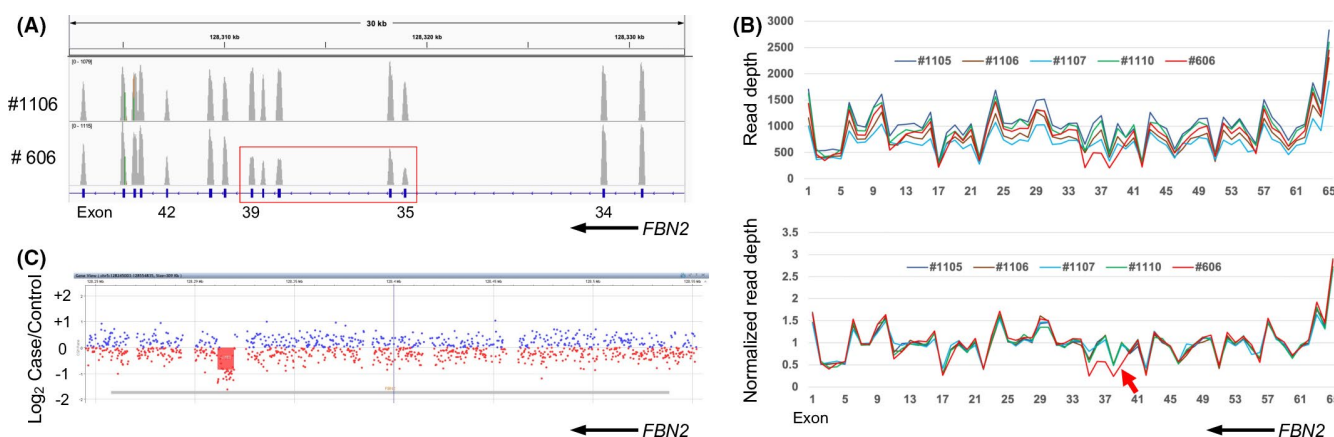

FIGURE 2 Copy number variation analysis. Results of CNV analysis obtained from the proband (II-3, #606). (A) Visual screening for CNVs by comparing IGV read coverage tracks. Upper panel shows a representative normal depth of coverage (*doc*) pattern, and the lower panel shows low-height *doc* patterns in the red enclosed part. (B) (upper panel) Read depth (RD) plot throughout the *FBN2* gene of five samples with close collection dates. (lower panel) RD for each was normalized by dividing it by the average of all RDs of the gene. Arrow indicates a marked decline in CNV-suspected region. (C) Array-CGH. The horizontal axis represents the nucleotide position. The vertical axis represents $\log_2$ (case/reference signal intensities on array-CGH). Dots with $\log_2$ (case/reference signal intensities) >0 are indicated in blue, and those <0 are indicated in red. The red-shaded area is a significant CNV region called by the Agilent CytoGenomics software
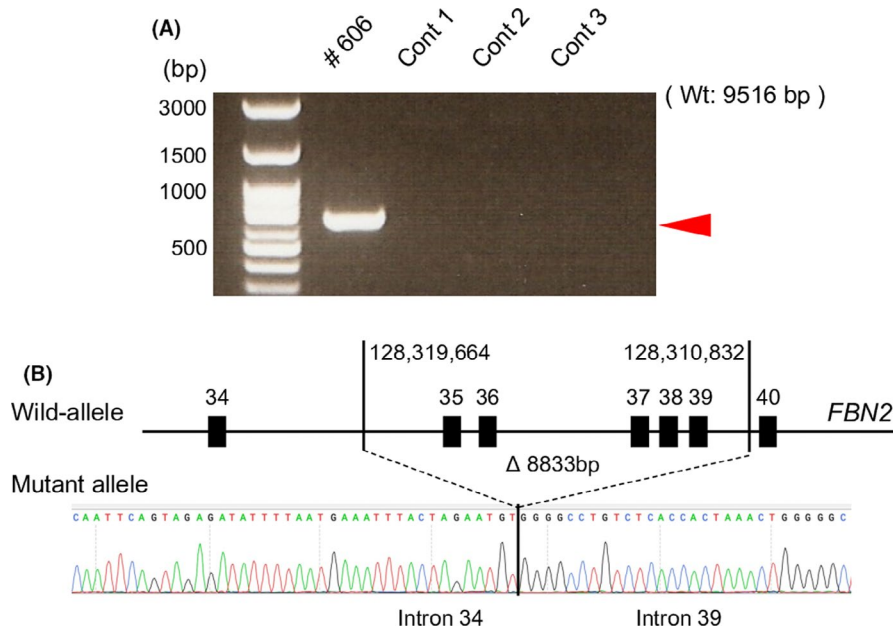
FIGURE 3 CNV breakpoint analysis. (A) Breakpoint analysis using PCR of the proband. Using primers flanking the breakpoint as described in the Methods section, the deleted allele (red arrow) was preferentially amplified over the larger normal allele in the proband. (B) Nucleotide sequences of the breakpoints and alignment with reference genomic sequence

from public variant databases, such as the Human Gene Mutation Database (HGMD®) (hgmd.cf.ac.uk/ac/index.php) or ClinVar (ncbi.nlm.nih.gov/clinvar/), but was predicted as deleterious by PROVEAN analysis. The proband and her second daughter were diagnosed with CCA, based on a constellation of her clinical features and the result of genetic analysis.

4 | DISCUSSION

In this report, we described a familial case of CCA with a novel heterozygous deletion of exons 35–39 in *FBN2* gene. The proband showed marfanoid habitus and mild camptodactyly without having aortic dilatation, suggestive of CCA, but neither Sanger sequencing nor routine NGS analysis could detect any putative causal *FBN2* variants. The CNV analysis finally identified the causative CNV as missing exons 35–39 in *FBN2*, in which as a screening method to predict CNV, visual comparison of the *doc* patterns of NGS panel testing data using IGV browser was valuable, making subsequent array-CGH analysis more efficient and smooth.

FBN2 is the only gene known to be associated with CCA, and most *FBN2* pathogenic variants cluster in exons 22–36, a middle part, and pathogenic variants are evenly distributed as missense and splice-site variants.[2] Several previous studies have demonstrated that whole gene deletion,[12–14] the duplication of exon 23,[15] and intragenic multiexon deletions[4,16] were also responsible for the development of CCA. However, the significance of additional CNV analysis in CCA after the routine NGS sequencing has not yet been established.

Multiplex ligation-dependent probe amplification (MLPA) and array-CGH are the gold standard methods in genotyping CNV, but still time-consuming and expensive approach if the number of exons and/or genes of interest become larger, and systematic evaluation of CNV is not routinely conducted in MFS-related disorders. However, systematic, accurate assessment of CNV using whole exome sequence and data from targeted gene panels is also still challenging due to issues intrinsic to the technology, including short read lengths and GC-content bias.[17,18] RD-based methods, which compare the observed and expected number of mapped reads in a genomic interval, suffer from a high proportion of false-positive predictions, especially when detecting small CNVs spanning only one or a few exons. Recently, we have successfully identified seven exonic CNVs in *FBN1* ($n = 6$) and *TGFB2* ($n = 1$) in patients with syndromic aortopathy *via* visual review of coverage (*doc*) patterns of NGS panel testing data using the IGV browser.[5] In the present study, we performed the CNV screening using such a simple methodology in a patient with suspected MFS and related disorders, and the subsequent array-CGH and breakpoint mapping by PCR confirmed the heterozygous deletion of exons 35–39 in *FBN2* as we expected.

In conclusion, we described a Japanese familial case of CCA with a novel heterozygous deletion affecting exons 35–39 in *FBN2*. If routine NGS sequencing is negative in patients with clinically diagnosed CCA, CNV analysis should be incorporated into the clinical diagnostic assessment, which would be valuable for the genetic diagnosis and counseling for family members, as well as the identification of the disease mechanism.

CONFLICT OF INTEREST

The authors declare no conflict of interest.

AUTHOR CONTRIBUTIONS

Hiroki Yagi (HY), Hiroshi Takiguchi (HT), Norifumi Takeda (NT), Ryo Inuzuka, and Yuki Taniguchi were directly involved in management of the case. HY, HT, and NT performed a visual inspection of copy number variation and prepared manuscript. Kristine Joyce Porto, Hiroyuki Ishiura, and Jun Mitsui performed array-CGH analysis. Hiroyuki Morita and Issei Komuro revised the manuscript critically for important intellectual content. All authors approved the content of the manuscript and confirmed the accuracy or integrity of any part of the work.

ETHICAL APPROVAL

The genetic analysis was approved by the University of Tokyo Hospital ethics committee (G-1538), and this case report was conducted in accordance with Declaration of Helsinki.

CONSENT

Written informed consent was obtained from the patient to use the data and pictures, and publish this report in accordance with journal's patient consent policy.

DATA AVAILABILITY STATEMENT

The data that support the findings of this study are available on request from the corresponding author. The data are not publicly available due to privacy or ethical restrictions.

ORCID

Norifumi Takeda https://orcid.org/0000-0003-4818-3347

REFERENCES

1. Callewaert BL, Loeys BL, Ficcadenti A, et al. Comprehensive clinical and molecular assessment of 32 probands with congenital contractural arachnodactyly: report of 14 novel mutations and review of the literature. *Hum Mutat*. 2009;30(3):334-341.
2. Frederic MY, Monino C, Marschall C, et al. The FBN2 gene: new mutations, locus-specific database (Universal Mutation Database FBN2), and genotype-phenotype correlations. *Hum Mutat*. 2009;30(2):181-190.
3. Takeda N, Morita H, Fujita D, et al. Congenital contractural arachnodactyly complicated with aortic dilatation and dissection: case report and review of literature. *Am J Med Genet A*. 2015;167A(10):2382-2387.
4. Meerschaut I, De Coninck S, Steyaert W, et al. A clinical scoring system for congenital contractural arachnodactyly. *Genet Med*. 2020;22(1):124-131.
5. Takeda N, Inuzuka R, Yagi H, et al. Clinical impact of copy number variation on the genetic diagnosis of syndromic aortopathies. *Circ Genom Precis Med*. 2021;14(4):e003458.
6. Robinson JT, Thorvaldsdottir H, Winckler W, et al. Integrative genomics viewer. *Nat Biotechnol*. 2011;29(1):24-26.
7. Plagnol V, Curtis J, Epstein M, et al. A robust model for read count data in exome sequencing experiments and implications for copy number variant calling. *Bioinformatics*. 2012;28(21):2747-2754.
8. Barrett MT, Scheffer A, Ben-Dor A, et al. Comparative genomic hybridization using oligonucleotide microarrays and total genomic DNA. *Proc Natl Acad Sci USA*. 2004;101(51):17765-17770.
9. Untergasser A, Cutcutache I, Koressaar T, et al. Primer3–new capabilities and interfaces. *Nucleic Acids Res*. 2012;40(15):e115.
10. Loeys BL, Dietz HC, Braverman AC, et al. The revised Ghent nosology for the Marfan syndrome. *J Med Genet*. 2010;47(7):476-485.
11. Roman MJ, Devereux RB, Kramer-Fox R, O'Loughlin J. Two-dimensional echocardiographic aortic root dimensions in normal children and adults. *Am J Cardiol*. 1989;64(8):507-512.
12. Ansari M, Rainger JK, Murray JE, et al. A syndromic form of Pierre Robin sequence is caused by 5q23 deletions encompassing FBN2 and PHAX. *Eur J Med Genet*. 2014;57(10):587-595.
13. Inbar-Feigenberg M, Meirowitz N, Nanda D, Toi A, Okun N, Chitayat D. Beals syndrome (congenital contractural arachnodactyly): prenatal ultrasound findings and molecular analysis. *Ultrasound Obstet Gynecol*. 2014;44(4):486-490.
14. Courtens W, Tjalma W, Messiaen L, et al. Prenatal diagnosis of a constitutional interstitial deletion of chromosome 5 (q15q31.1) presenting with features of congenital contractural arachnodactyly. *Am J Med Genet*. 1998;77(3):188-197.
15. Gupta PA, Putnam EA, Carmical SG, et al. Ten novel FBN2 mutations in congenital contractural arachnodactyly: delineation of the molecular pathogenesis and clinical phenotype. *Hum Mutat*. 2002;19(1):39-48.
16. Lavillaureix A, Heide S, Chantot-Bastaraud S, et al. Mosaic intragenic deletion of FBN2 and severe congenital contractural arachnodactyly. *Clin Genet*. 2017;92(5):556-558.
17. Zhao L, Liu H, Yuan X, Gao K, Duan J. Comparative study of whole exome sequencing-based copy number variation detection tools. *BMC Bioinformatics*. 2020;21(1):97.
18. Moreno-Cabrera JM, Del Valle J, Castellanos E, et al. Evaluation of CNV detection tools for NGS panel data in genetic diagnostics. *Eur J Hum Genet*. 2020;28(12):1645-1655.